Received: 28 January 2016 | Revised: 2 August 2016 | Accepted: 25 February 2017

DOI: 10.1002/stc.2016

RESEARCH ARTICLE

WILEY

Pipeline internal corrosion monitoring based on distributed strain measurement technique

Tao Jiang[1] | Liang Ren[1] | Zi-guang Jia[2] | Dong-sheng Li[1] | Hong-nan Li[1,3]

[1] School of Civil and Hydraulic Engineering, Dalian University of Technology, Dalian, 116024, China

[2] School of Ocean Science and Technology, Dalian University of Technology, Panjin, 124221, China

[3] School of Civil Engineering, Shenyang Jianzhu University, Shenyang, 110168, China

Correspondence
Liang Ren, School of Civil and Hydraulic Engineering, Dalian University of Technology, Dalian, China.
Email: renliang@dlut.edu.cn

Funding Information
Fundamental Research Funds for the Central Universities, Grant/Award Number: DUT15YQ107; Fund of the National Natural Science Foundation of ChinaGrant/Award Numbers: 51327003 and 51421064; National Basic Research Program of China (973 Program), Grant/Award Number: 2015CB060000

Summary

Pipeline corrosion is an important issue that threatens the pipeline safety operation; therefore, the corrosion monitoring is essential. Based on the optical frequency domain reflectometry technology, which features distributed strain measurement with high resolution and high precision, a new method of pipeline internal corrosion monitoring is proposed to simultaneously locate corrosion and to evaluate corrosion severity. To verify the effectiveness and accuracy of this method, a series of tests were conducted including uniform corrosion test and local corrosion tests. These test results demonstrate that the corrosion location and corrosion severity evaluation can be achieved via the proposed distributed strain measurement, providing a valuable approach for pipeline corrosion monitoring.

KEYWORDS

corrosion, hoop strain, monitoring, pipeline, OFDR

1 | INTRODUCTION

Pipeline is an efficient way to transport fluid, specially, petroleum and its products. The key problem with pipeline is leakage. Even a small amount of leakage may cause a large damage to the environment or can put people on a great risk.[1] Corrosion is one of the major contributors to accidental events in pipelines.[2] Pipeline corrosion includes external corrosion and internal corrosion. In order to prevent the external corrosion induced by the corrosive medium, the external surface of pipeline is traditionally protected by a protective system that is comprised with insulation and cathodic protection. However, due to the joint action of fluid flushing, corrosive medium, and microorganism, it is hard to prevent internal corrosion. Thus, detecting internal corrosion and assessing its safety performance become an important research topic owing to its technical and economical impacts.[3]

With the advantages of high precision, magnetic flux leakage,[4] radiography testing,[5] and ultrasonic testing[6] are widely used in pipeline corrosion detection. However, these methods are not suitable for the corrosion detection in real time. Pipeline corrosion monitoring, focusing on detecting the initiation of corrosion and assessing the pipe safety performance, has become an important research topic.[7] Some representative corrosion-monitoring techniques are summarized as follows. Electrochemical impendence spectroscopy, a relative mature method for measuring corrosion rate, has been successfully applied to the study of corrosion systems.[8,9] Linear polarization resistance[10] is a particularly useful technique to rapidly identify corrosion. A microsized linear polarization resistance sensor was invented to provide real-time measurements of metal loss and corrosion rate.[11] Electrical resistance technique is to provide a direct measurement of metal loss and corrosion rate.[12] However, for oil and gas pipeline monitoring, the use of electric sensors will cause many potential dangers to the pipeline safety operation.[13] Moreover, long distances between the corrosion points and the monitoring station make electronic- and

electromagnetic-based corrosion sensors inappropriate for monitoring these pipelines.

Optic-sensing technologies, with their superior immunity to electromagnetic interference, long-distance transmission, high accuracy, and reliability,[14] are particularly attractive for using in harsh environments, under high temperatures, pressures, and electromagnetic fields. Considering their superior abilities, optic-sensing technologies have received increasing attention in the study of corrosion monitoring. Bennett et al.[15] designed a prototype optical fiber sensor for monitoring corrosion on large steel structures. On the basis of evanescent wave phenomena, Fuhr et al.[16] introduced a fiber optic corrosion-sensing system allowing for the detection of general corrosion on and within materials. Martins-Filho et al.[17] proposed and demonstrated an optical fiber sensor for testing the corrosion process in metal using the optical time domain reflectometry (OTDR) technique. Zou et al.[18] developed a brillouin-scattering-based fiber optic distributed strain sensor and applied to measure the longitudinal and hoop strain in a steel pipe model with wall-thinning defects; the locations of structural defects were found and distinguished. Based on an optic fiber inscribed with long-period fiber gratings, Huang et al.[19] proposed a corrosion sensor to monitor the corrosion information of the pipeline samples in real time remotely. Hu et al.[20] developed an Fe-C-coated fiber Bragg gratings (FBGs) for steel corrosion monitoring by measuring strains in the radius direction when wrapped on the steel bar. Ren et al.[21] designed an FBG hoop-strain sensor that can be used to measure pipeline uniform corrosion levels. Each of the above methods has its own advantages and limitations. For example, commercially available techniques based on Raman and Brillouin scatter measurements typically employ OTDR has found wide applications for long-distance distributed measurement due to its large dynamic range, whereas their measurement resolution is usually in order of meter to tens of meter, which is not well suited for applications that require high resolution. Because the pipeline corrosion detection requires high resolution, OTDR-based methods are generally not suitable for such a task.

According to the survey conclusion conducted by Wang et al.,[22] the most direct phenomenon caused by corrosions is the reduction of the wall thickness of a pipeline, and, as a result, the hoop strain variation can reflect the change of wall thickness directly. Optical frequency domain reflectometry (OFDR) combined with high-performance digital signal processors is used to measure distributed strain with millimeter scale resolution and microstrain measurement precision,[23] providing an effective method for pipeline corrosion monitoring. In this paper, a new method based on OFDR technique is proposed to monitor pipeline internal corrosion, including corrosion localization and corrosion severity evaluation. This method utilizes an optical distributed sensor interrogator based on OFDR technique to monitor the corrosion of the pipeline, covering both uniform corrosion and local corrosion. To verify the correctness of the monitoring theory, an analysis was carried out by using finite element (FE) method in Abaqus.

2 | MONITORING THEORY OF PIPELINE INTERNAL CORROSION

The internal pressure is considered to be a known quantity for the long-term service of pipeline. Due to the growth of pipeline corrosion, the wall thickness of the pipeline will be reduced.

2.1 | Uniform corrosion

For uniform corrosion, corrosion proceeds at approximately the same rate over the whole surface, which makes the pipeline expands uniformly under working pressure. According to the principle of materials mechanics, the relationship between the hoop strain and the wall thickness can be obtained:

$$\varepsilon = \frac{PD}{2Et}, \tag{1}$$

where ε is the hoop strain of the pipeline; P is the internal pressure of the pipeline; E is the Young's modulus; and t is the wall thickness of the pipeline. P and D are constants because pipelines usually work in the condition of steady pressure, and the diameter of the pipeline is a constant in practical use. Based on this theory, the reduction of the wall thickness can be obtained by monitoring the change of the hoop strain.

2.2 | Local corrosion

With regard to local corrosion, a pipeline loses a certain percentage of wall thickness when a corrosion defect occurs. At the same time, a larger strain occurs in the defective area and its surrounding region under the certain internal pressure.[18] An example of local corrosion analysis based on FE method is conducted to explain the abovementioned phenomenon. The FE pipeline model is shown in Figure 1. In the FE model, the length of pipe is $L = 1{,}280$ mm, 4 times larger than the pipe diameter $D = 327$ mm. The radian of the local corrosion area is $\pi/6$ along the pipe's circumference, and the length of the corrosion area along the axial direction is 80 mm. The influence of the boundary condition on the force can be neglected because the local corrosion exists in the middle of the pipe. The FE pipe model was loaded with internal pressure $P = 1$ MPa.

It can be observed from Figure 2 that the hoop strain of corrosion area (red zone) is larger than that of the corrosion-free area (green zone). Meanwhile, there are two symmetric strain mutation areas at both sides of the corrosion

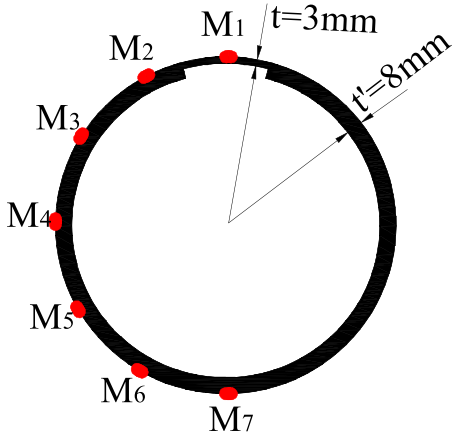

FIGURE 1 Diagram of local corrosion and strain measurement point

area along the circumferential direction. To illustrate the strain distribution of this case, 7 test points M1~M7 (shown in Figure 1) are used to represent the hoop strain variation. Please note that M1 is the measure point that exactly locates at the corrosion area and M2 locates at the strain mutation area. The hoop strains of the 7 single points were extracted and presented in Table 1. Obviously, the maximum strain appears at M1 point, where is the center of the corrosion area, whereas the hoop strain of points M3–M7 are same as those of the corrosion-free pipeline, indicating that the influence area of the local corrosion is limited. Because of the abrupt change of the cross section at the border of the corrosion area, the hoop strain abruptly decreases around M2 point. It can be concluded that the local corrosion directly causes the hoop strain concentration on the corrosion area and the local corrosion can be identified via the hoop strain distribution.

3 | SENSOR INSTALLATION AND MEASUREMENT SYSTEM

3.1 | Sensor installation

In the tests, optic fibers were bonded along the circumferential central line of each segments of the steel pipe to avoid the influence of boundary condition. Before bonding the optical fiber, a sander and abrasive paper were used to process the area for sensor installation, providing a smooth and uniform surface around its circumference. After the polishing, the surface was cleaned by cotton immersed in alcohol. Then the prestrained optical fibers were bonded onto the surface with the cyanoacrylate adhesive.

TABLE 1 Hoop strain of point M1–M7

Location	M1	M2	M3	M4	M5	M6	M7
Hoop strain (με)	148.5	47.3	67.2	67.8	67.8	68.3	67.8

3.2 | Measurement system

Distributed strain data were acquired from the sensing optic fiber via an OFDR-based interrogator that can achieve 2.56 mm sensor spacing, 5.12 mm gage length, and ±5 microstrains measurement precision. The interrogator uses swept-wavelength interferometry to measure the Rayleigh backscatter as a function of position in the optical fiber. Physical changes (such as temperature and strain) to the sensor create a measurable change to how light is scattered from locations along the optical fiber.[24] Thus, position of the sensing fiber can be used to measure the strain and temperature, similar to the optic fiber engraved with continuous distributed FBG sensors.

The optic fiber was connected to an interrogator that sent data via an Ethernet to a PC. Data were acquired for each of the installed optic fiber sensors at a rate of 10 Hz. A water pump with 2.5 MPa maximum pumping pressure was used to provide the pressurized condition to simulate the working environment of a practical pipeline. A pressure sensor was installed in the pipeline model to measure the internal pressure. The schematic diagram of measurement system is shown in Figure 3. All the tests were conducted in a laboratory setting with small fluctuation; therefore, the influence of temperature on strain measurement can be neglected.

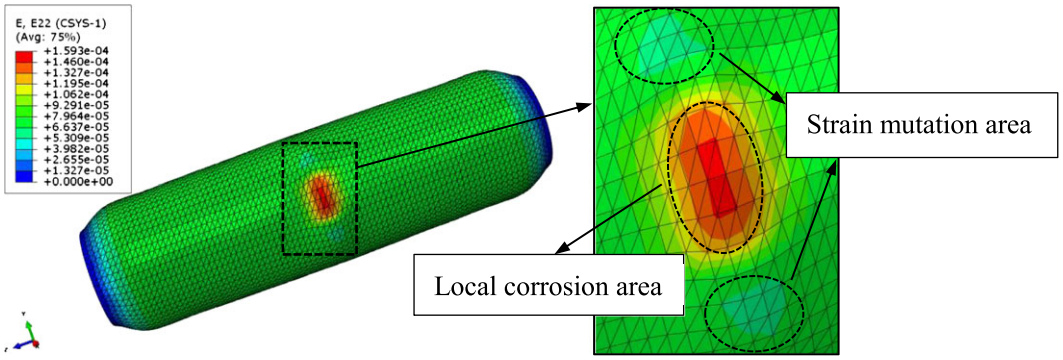

FIGURE 2 Hoop strain nephogram of the numerical pipe model

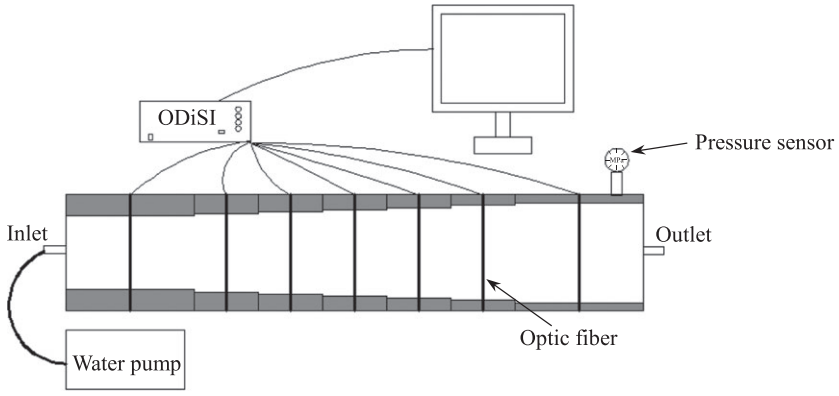

FIGURE 3 Schematic diagram of the optical frequency domain reflectometry measurement system

4 | SENSOR CALIBRATION AND REPEATABILITY

To characterize the working performance of the optic fiber, a series of calibration tests were conducted on a steel plate, whose Young's modulus value was 2.06×10^5 MPa. The cross-sectional area of the steel plate is a rectangle (30 mm × 5.7 mm), and the surface of the steel plate was cleaned carefully before bonding the optic fiber. As shown in Figure 4, five test segments 1–5 of one optic fiber, with length of 20 cm each, were bonded to the steel plate to measure the strain distribution. Segments 1 and 5 are located at both sides of the steel plate, and Segment 3 is located in the middle of the steel plate, whereas the remaining segments of the optic fiber were not bonded to the steel plate. Tensile tests of the steel plate were carried out on a universal material-testing machine shown in Figure 4. In the tests, the steel plate was clamped firmly at both ends and loaded continuously from 0 KN to 16 KN at interval of 2 KN. The strain distribution of Number 3 optic fiber is shown in Figure 5. Theoretically, for a uniform plate, the strain distribution of each loading step should be a horizontal line. It can be seen from Figure 5 that the measured strain distribution agrees with the theoretical strain distribution (the straight lines shown in Figure 5) of the steel plate under the tensile load.

To evaluate the strain measurement performance, the strain variation under every loading step of a specific

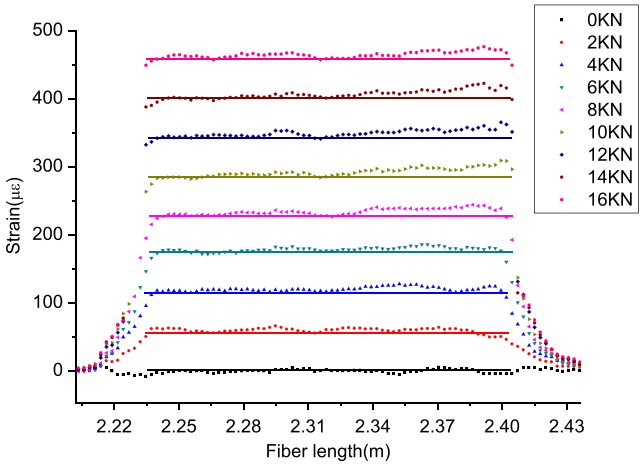

FIGURE 5 Strain distribution of Number 3 optic fiber

measuring point (in the middle of No. 3) was extracted and shown in Figure 6, as well as the theoretical results. The coefficient of linear correlation is more than 0.999, verifying the test results has good linearity. Excellent agreement between theory and experiment was observed at each load step. All the results demonstrated that the optic fiber works well on steel materials.

For investigating the performance of optic fiber in the hoop strain measurement, the calibration tests were carried out on a segment of DN250 pipe prototype with 273 mm diameter and 8 mm wall thickness (shown in Figure 7). The optic fiber was bonded in the middle of the test pipe along

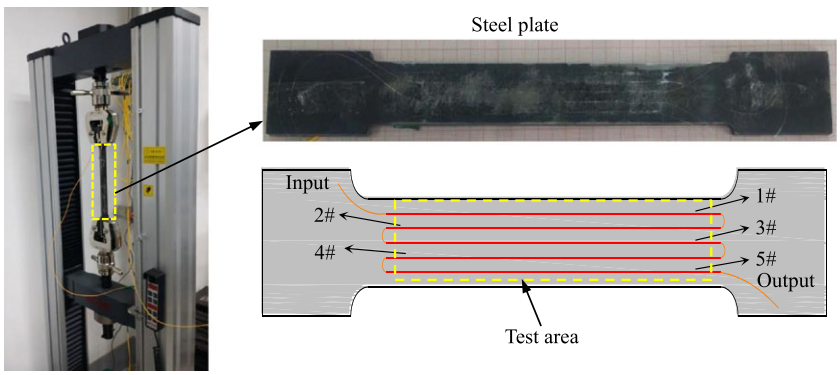

FIGURE 4 Calibration experiment using universal material test machine

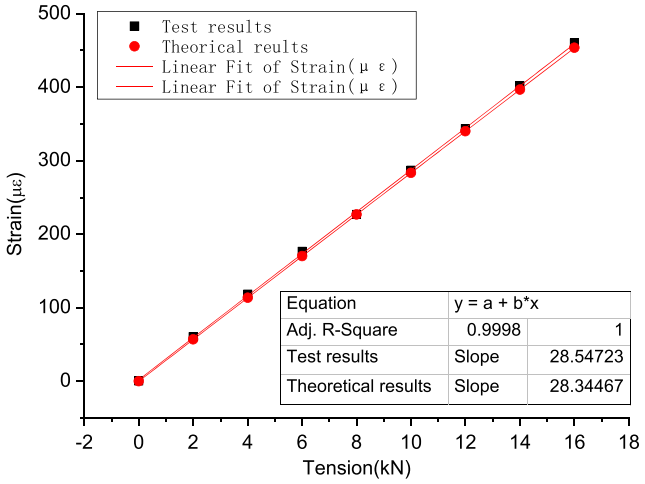

FIGURE 6 Sensor calibration result

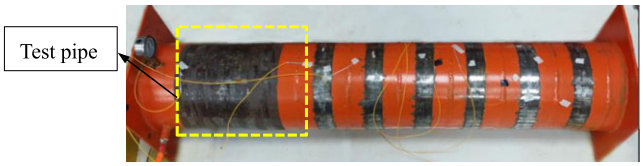

FIGURE 7 Calibration test pipe

the circumferential direction and covered the whole circle. The internal pressure was loaded step by step continuously from 0 to 1 MPa at interval of 0.2 MPa.

Figure 8 shows the hoop strain variation of the pipe during the incremental internal pressure. The measurement part of the optic fiber (from 1.17 to 2.12 m) was bonded to the outer surface of the pipe. Similar to the tests on the steel plate, the hoop strain distribution of each loading step is supposed to be a flat line. However, some strain fluctuations occur due to the wall thickness inhomogeneity, obviously in relative higher pressure condition. The hoop strain variation of 3 points were extracted, presented in Figure 9. It illustrates

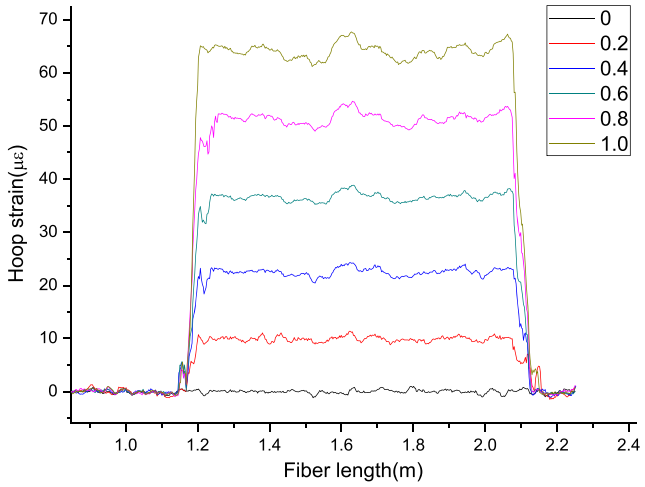

FIGURE 8 Hoop strain distribution

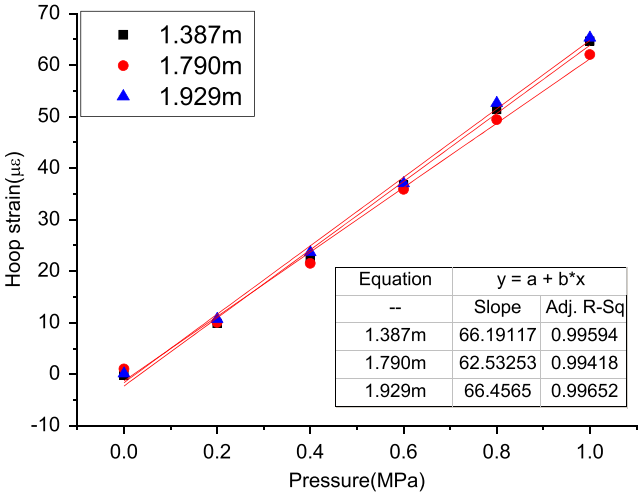

FIGURE 9 Result of optic fiber calibration test

that the hoop strain recorded by the optic fiber sensor is linear to the internal pressure from the first to the fifth loading conditions, demonstrating that the optic fiber is suitable for pipeline hoop strain measurement.

Repeatability is an important aspect of any sensor, especially in terms of long-term monitoring of long-distance pipeline. Thus, the cyclic-loading test was conducted on the abovementioned model pipe. The pipe was pressurized repeatedly from 0 to 1 MPa, during which the strain variation of each loop was recorded and presented in Figure 10. The results demonstrate that the behavior of optic fiber sensor is steady and repeatable in the repeatability test.

5 | EXPERIMENTAL RESULTS

5.1 | Uniform corrosion test

The uniform corrosion model is consisted of seven segments with the same outside diameter (273 mm) but different wall thickness (e.g., 6.0, 5.0, 4.6, 4.2, 3.8, 3.4, and 3.0 mm) as denoted in Figure 11. The different wall thicknesses of these

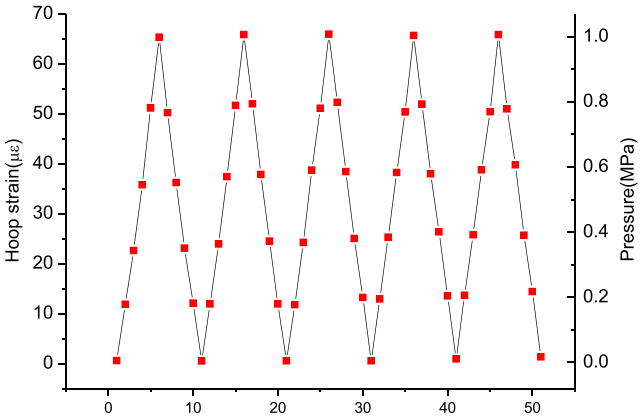

FIGURE 10 Cyclic loading test at position of 1.40 m

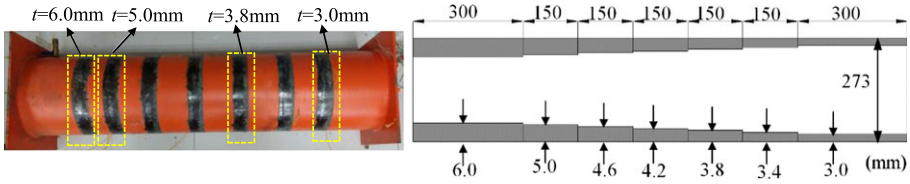

(a)Pipe model (b)Cross-sectional view of the pipeline model

FIGURE 11 The steel pipe model used for simulating different uniform corrosion levels

pipes simulated the different uniform corrosion severity of a pipeline internal wall. The two segments at both ends were manufactured twice the length of the middle segments to diminish the influence of the boundary effect. Optic fibers were bonded in the center of the outer surface of four pipe sections, with wall thickness of 3, 3.8, 5.0, and 6.0 mm.

Figure 12 shows the hoop strain distributions of the four segments under the internal pressure of 0.7 MPa. By comparing the four test results, it can be seen that the hoop strain increases with the decrease of the wall thicknesses. This phenomenon indicates that the above monitoring theory based on hoop strain measurement is applicable for uniform corrosion pipeline. In practice, the initial hoop strain distribution of a corrosion-free pipeline can be acquired and set as the reference strain. Thus, the corrosion is predicable when the strain is detected to be larger than the reference strain. Furthermore, the reduction magnitude of wall thickness caused by uniform corrosion can be also estimated. Because of measurement noise in actual environment and the inhomogeneous wall thickness, some strain fluctuations occur in the test results.

5.2 | Local corrosion model with different corrosion scopes

The growth of local corrosion reduces the wall thickness, simultaneously causing the corrosion area increase.[25] Hence, a local corrosion model (shown in Figure 13) was

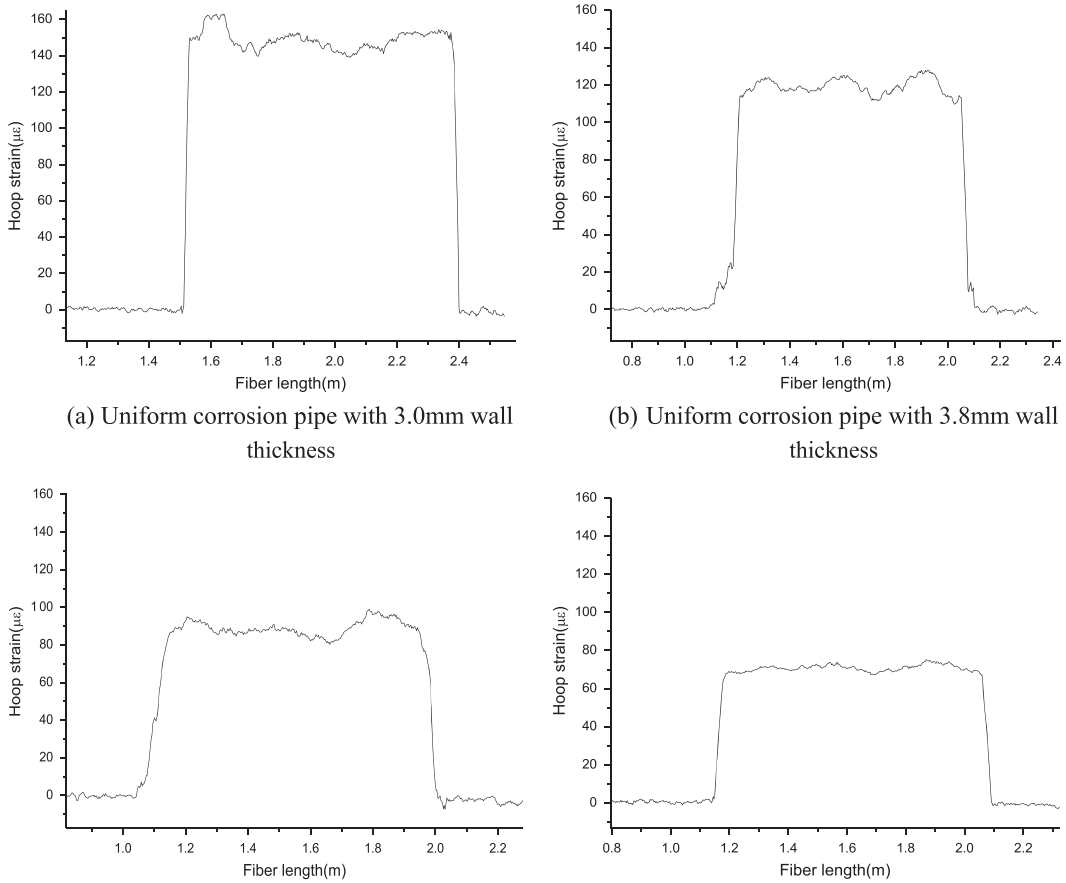

(a) Uniform corrosion pipe with 3.0mm wall thickness

(b) Uniform corrosion pipe with 3.8mm wall thickness

(c) Uniform corrosion pipe with 5.0mm wall thickness

(d) Uniform corrosion pipe with 6.0mm wall thickness

FIGURE 12 Hoop strain distribution of the uniform corrosion model

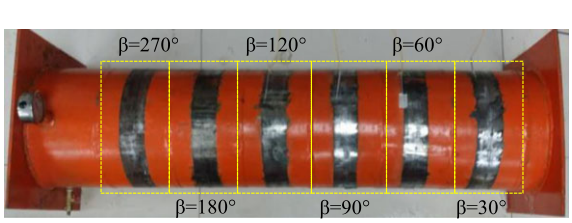

(a) Steel pipe model

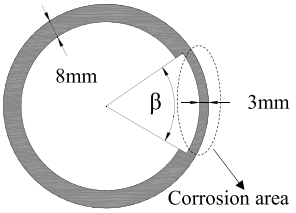

(b) Cross section of steel pipe model

FIGURE 13 The steel pipe model used for simulating different local corroded scopes

fabricated to simulate the pipe with different corrosion scope. The steel pipe model is composed of six segments with different defect angles (e.g., 30°, 60°, 90°, 120°, 180°, and 270°), but with the same wall thickness at these defect areas. The increasing defect angle represents the growing corrosion scope. Four optic fibers were bonded on the outer surface of the four segments with defect angle of 30°, 60°, 90°, and 120°.

Figure 14 clearly presents the tested strain distribution of the four segments with different defect angles. Owing to the steps on the cross section (shown in Figure 13b), strain sudden drop occurred at the boundary of the defect region. Thus, the defect region can be identified by the strain sudden drop. To help analyze the results, the abscissas of the two minimum hoop strain points were taken as the starting point and ending point of the defect regions, respectively. Then the angles of the detected defect regions were calculated and presented in Table 2. Meanwhile, the error ratio η is defined to represent the accuracy of defect angle detection.

$$\eta = \frac{|\beta - \alpha|}{\beta} \times 100\%, \tag{2}$$

where β and α denote the real value and the measurement value of the defect angle, respectively. It can be seen from

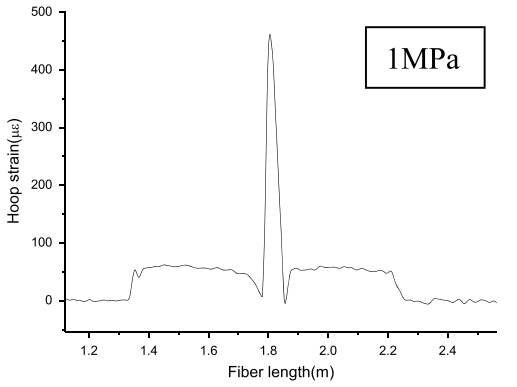

(a) Local corrosion pipe with 30° defect angle

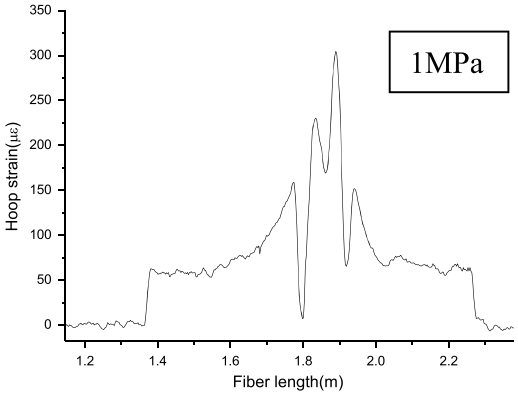

(b) Local corrosion pipe with 60° defect angle

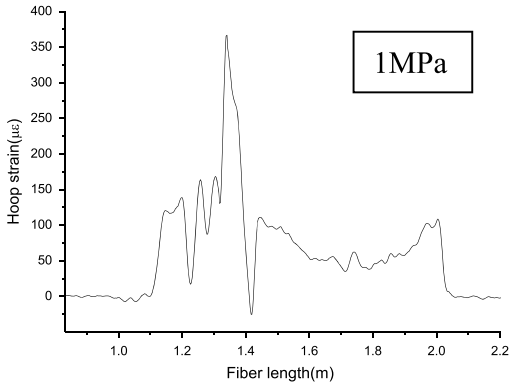

(c) Local corrosion pipe with 90° defect angle

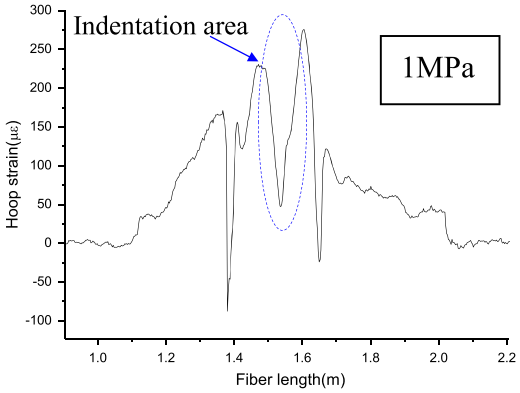

(d) Local corrosion pipe with 120° defect angle

FIGURE 14 Hoop strain distribution of local corrosion model with different defect angle

TABLE 2 Test results of the local corrosion model with different defect angle

Defect angle (β)	Start point (m)	End point (m)	Test angle (α)	Error ratio (η; %)
30°	1.781	1.855	31.1	3.67
60°	1.793	1.926	57.5	4.17
90°	1.218	1.425	87.0	3.33
120°	1.376	1.654	116.8	2.68

Table 2 that the detected angles agree well with the actual ones, and all the error ratios are less than 5%, indicating that the corrosion scope can be identified by the two minimum hoop strain points. Additionally, strain concentration occurs in the local corrosion area. Therefore, the local corrosion can be located because the corresponding position of the two minimum hoop strain points and the strain concentration can be detected by the hoop strain distribution diagram. In summary, the proposed OFDR-based distributed strain measurement technique can evaluate the corrosion scope and determine the corrosion location.

There exists some indentations on the surface of the test model, and some of them cannot be polished. Because one such indentation locates at the defect area of the pipe with 120° defect angle (shown in Figure 15), the optic fiber cannot be bonded uniformly on the surface, which directly causes the abrupt change of the test strain distribution, as shown in Figure 14d.

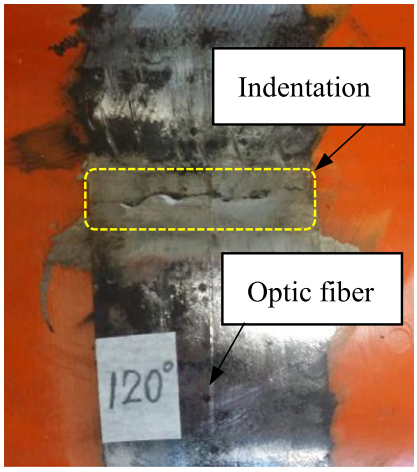

FIGURE 15 Indentation on the pipe outer surface

5.3 | Local corrosion model with different corrosion thickness

In order to investigate the performance of proposed optic fiber technique for local corrosion location and corrosion severity evaluation, a series of tests were conducted on the local corrosion model. This model is consisted of one corrosion-free segment and six segments with local corrosion, as shown in Figure 16a. To simulate the different severity of local corrosion generating in the internal wall, 90° arc-shaped defects with different depth were wire cut and removed from the pipe's inner surface of each local corrosion section, as sketched in Figure 16b. The thicknesses of the six corroded pipe sections are 6.5, 4.5, 3.5, 2.8, 2.3, and 2.0 mm. Then optic fibers were mounted on the outer surface of the each segment to measure the hoop strain distribution.

To verify the repeatability of this distributed optical fiber for the local corrosion measurement approach, optic fiber was bonded to the pipe whose wall thickness of local corrosion area is 3.5 mm with two circles. It can be observed in Figure 17 that the strain variation tendency, including both the sudden changes and the fluctuations, is periodical within each circumference of 0.86 m, especially the absolute values of the strain peaks and valleys are approximately identical.

It can be seen that the similar hoop strain distribution appears in Figure 18a–d. For example, Figure 18a shows the strain field of the 2.0-mm depth-corrosion segment under different load levels. A segment of this optic fiber sensor from 2.17 to 2.38 m was located at the local corrosion area.

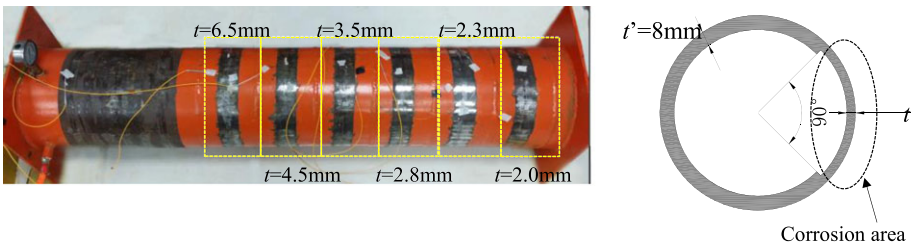

(a) Steel pipe model (b) Cross section of local corrosion pipe

FIGURE 16 The steel pipe model used for simulating different local corrosion levels

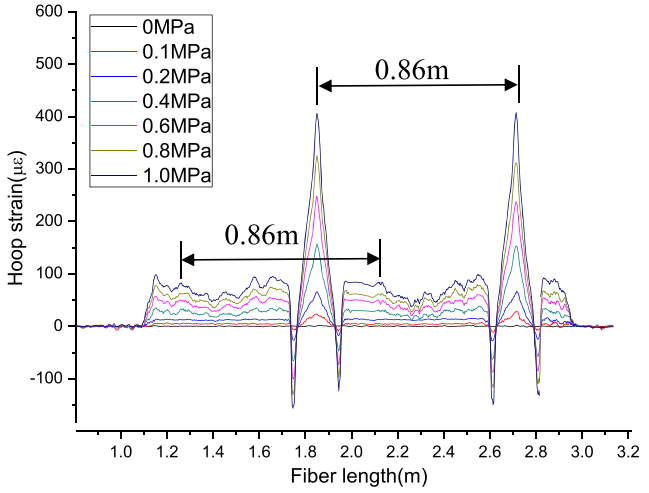

FIGURE 17 Hoop strain distribution of the local corrosion pipe with 3.5 mm wall thickness

Data measured with the optical fiber detect that strain concentrated in the local corrosion area. The greater the load level is, the more noticeable strain concentration phenomenon occurs. Even at low-load levels, the strain of local corrosion area is larger than that of the corrosion-free area. Owing to the influence of local corrosion, the hoop strain around local corrosion area is larger than those in other corrosion-free areas. Because there exists a step on the cross section between corrosion and corrosion-free area, as shown in Figure 16b, the hoop strain on the junction part turns from tensile strain to compressive strain abruptly.

The developing of local corrosion will directly cause the reduction of the wall thickness. The maximum hoop strain of the defect regions when loaded with 0.6 MPa inner pressure were extracted from the test results and presented in Table 3. It illustrates that the thicker the wall thickness is, the greater strain magnitude occurs. Therefore, the local

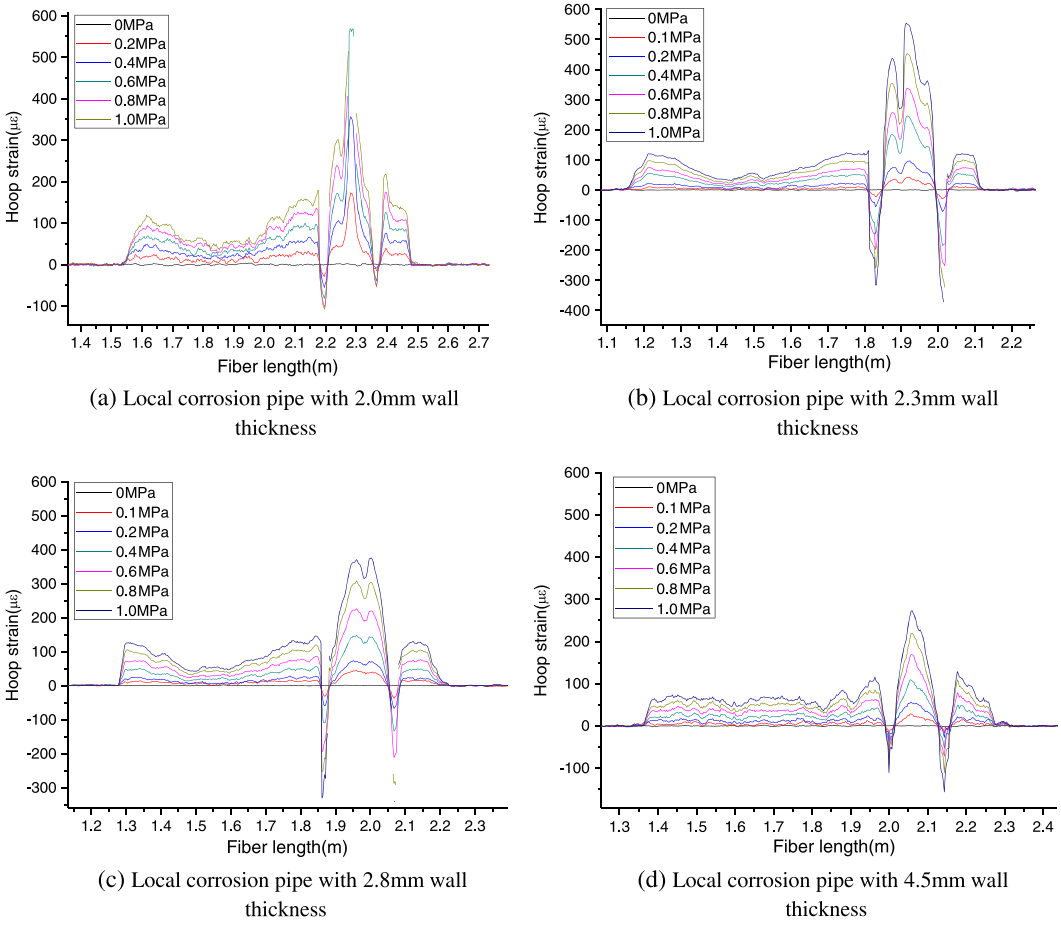

(a) Local corrosion pipe with 2.0mm wall thickness

(b) Local corrosion pipe with 2.3mm wall thickness

(c) Local corrosion pipe with 2.8mm wall thickness

(d) Local corrosion pipe with 4.5mm wall thickness

FIGURE 18 Hoop strain distribution of local corrosion model with different wall thickness

TABLE 3 The maximum hoop strain of different local corrosion areas

Wall thickness of local corrosion area (mm)	2.0	2.3	2.8	4.5
Maximum hoop strain (με)	566.1	338.4	222.7	168.7

corrosion severity can be evaluated via the OFDR-based distributed strain measurement technique.

Moreover, test results demonstrate that the increasing internal pressure can magnify the surface strain of the defect area, implying that this OFDR-based distributed strain-measuring technique can also be applied to detect and locate the internal wall damage of some pressure vessels by bonding the sensing fiber to the outer surface of the vessels.

Notwithstanding the corrosion morphology of practical pipeline is different with the above test models, the growing of corrosion defects will certainly induce concentration according to the test results and the numerical analysis. With the advantages of high sensitivity, good electrical insulation, and real-time measurement, the OFDR-based distributed stain measurement technique provides an effective approach for pipeline corrosion monitoring in engineering.

6 | CONCLUSIONS

Theoretical and numerical simulation results demonstrated that hoop strain distribution reflects the wall thickness variation induced by internal corrosion under certain inner pressure. The OFDR technique with its advantages in high-spatial resolution and high-precision strain measurement provides an effective approach for distributed strain measurement. Thus, a method based on hoop strain measurement was proposed to identify the pipeline internal corrosion. A series of simulated internal corrosion tests were conducted to verify the feasibility of this method. The tests include corrosion localization and corrosion severity assessment. From the above investigations, the following conclusions can be obtained:

1. For uniform corrosion, the variation of the distributed hoop strain can be used to evaluate the reduction of the pipeline wall thickness.
2. Strain concentration occurs on the local corrosion area, and the thinner the wall thickness is, the more noticeable strain concentration phenomenon occurs.
3. The influence range of strain concentration is determined by the local corrosion dimensions (depth and angle).
4. The OFDR-based distributed strain measurement has superior performance in the pipeline corrosion monitoring, including uniform corrosion level evaluation, local corrosion scale determination, and corrosion location.

Further investigation may focus on the assessment of the residual strength based on the distributed strain measurement. Meanwhile, the long-term stability of the distributed strain-based pipeline corrosion-monitoring method is another important issue that should be studied.

ACKNOWLEDGMENTS

This work has been supported by the 973 Program (Grant 2015CB060000 and 2015CB057704), the Science Fund for Creative Research Groups of the National Natural Science Foundation of China (Grant 51421064), the Fund of the National Natural Science Foundation of China (Grant 51327003, 51278084, and 51478080), and the Fundamental Research Funds for the Central Universities (DUT15YQ107). These grants are greatly appreciated.

REFERENCES

[1] C. A. Laurentys, C. H. M. Bomfim, B. R. Menezes, W. M. Caminhas, *Appl. Soft Comput.* **2011**, *11*(1), 1057.

[2] R. C. Tennyson, W. D. Morison, *Smart Structures and Materials. International Society for Optics and Photonics* **2006**; 61671C-61671C-13.

[3] T. Jiang, L. Ren, D. S. Li, X. Cheng, Z. G. Jia, *J. Optoelectron. Laser* **2015**, *26*(8), 1536.

[4] A. Joshi, L. Udpa, S. Udpa, A. Tamburrino, *Magn. IEEE Trans. Magn.* **2006**, *42*(10), 3168.

[5] K. Edalati, N. Rastkhah, A. Kermani, M. Seiedi, A. Movafeghi, *Int. J. Press. Vess. Pip.* **2006**, *83*(10), 736.

[6] A. Demma, P. Cawley, M. Lowe, A. G. Roosenbrand, B. Pavlakovic, *Ndt E Int.* **2004**, *37*(3), 167.

[7] Y. Huang, D. Ji, *Sens. Actuators B* **2008**, *135*(1), 375.

[8] R. P. V. Cruz, A. Nishikata, T. Tsuru, *Corros. Sci.* **1996**, *38*(8), 1397.

[9] X. Li, H. Castaneda, *Corrosion Eng. Sci. Tech.* **2015**, *50*(3), 218.

[10] G. Rocchini, *Corros. Sci.* **1999**, *41*(12), 2353.

[11] R. J. Connolly, D. Brown, D. Darr, J. Morse, B. Laskowski, *Eng. Asset Manag.-Syst. Prof. Pract. Cert.* **2015**, 673.

[12] S. Y. Li, Y. G. Kim, S. Jung, H. S. Song, S. M. Lee, *Sens. Actuators B* **2007**, *120*(2), 368.

[13] D. R. Sonyok, B. Zhang, J. Zhang, *Pipelines 2008—Pipeline Asset Management@ sMaximizing Performance of our Pipeline Infrastructure* **2008**.

[14] H. N. Li, D. S. Li, G. B. Song, *Eng. Struct.* **2004**, *26*(11), 1647.

[15] K. D. Bennett, L. R. McLaughlin, *Smart Structures & Materials' 95*. International Society for Optics and Photonics, **1995**, 48–59.

[16] P. L. Fuhr, T. P. Ambrose, D. R. Huston, A. P. McPadden, *Smart Structures & Materials' 95*. International Society for Optics and Photonics **1995**: 2–8.

[17] J. F. Martins-Filho, E. Fontana, J. Guimaraes, D. F. Pizzato, I. S. Coelho, *IEEE Sensors* **2007**, *2007*, 1172.

[18] L. Zou, O. Sezerman, W. Revie, *Nace International Corrosion* **2008**.

[19] Y. Huang, X. Liang, F. Azarmi, *Pipelines* **2014**, *2014*, 1502.

[20] W. Hu, H. Cai, M. Yang, X. Tong, C. Zhou, W. Chen, *Corros. Sci.* **2011**, *53*(5), 1933.

[21] L. Ren, Z. G. Jia, H. N. Li, G. B. Song, *Opt. Fiber Tech.* **2014**, *20*(1), 15.

[22] G. L. Wang, N. Ma, Y. Chen, *Nucl. Power Eng.* **2012**, *33*, 1.

[23] J. Bos, J. Klein, M. Froggatt, E. Sanborn, D. Gifford, *SPIE Optical Engineering+ Applications*. International Society for Optics and Photonics **2013**: 887614-887614-15.

[24] Luna ODiSI Optical distributed sensor interrogator user guide.

[25] R. K. Ginzel, W. A. Kanters, *NDT. net* **2002**, *7*(07), 1435.

How to cite this article: Jiang T, Ren L, Jia Z, Li D, Li H. Pipeline internal corrosion monitoring based on distributed strain measurement technique. *Struct Control Health Monit*. 2017;24:e2016. https://doi.org/10.1002/stc.2016